Available online at www.sciencedirect.com
ScienceDirect
Trans. Nonferrous Met. Soc. China 31(2021) 1322−1338
Transactions of Nonferrous Metals Society of China
www.tnmsc.cn

Effect of pre-rolling path on mechanical properties of rolled ZK60 alloys

Bo SONG[1], Zhi-wen DU[1], Qing-shan YANG[2], Ning GUO[1], Sheng-feng GUO[1], Jin-cheng YU[3], Ren-long XIN[4]

1. School of Materials and Energy, Southwest University, Chongqing 400715, China;
2. School of Metallurgy and Materials Engineering, Chongqing University of Science and Technology, Chongqing 401331, China;
3. School of Mechanical Technology, Wuxi Institute of Technology, Wuxi 214121, China;
4. College of Materials Science and Engineering, Chongqing University, Chongqing 400044, China

Received 21 May 2020; accepted 4 February 2021

Abstract: Pre-cold rolling with low reductions (<3%) was used to improve the mechanical properties of rolled ZK60 plates. The effects of rolling path on mechanical properties were investigated in detail. Both pre-cold rolling along the transverse direction (TD) and pre-cold rolling along the normal direction (ND) can increase the yield strength. However, pre-cold rolling along the TD is more effective than pre-cold rolling along the ND in improving the comprehensive mechanical properties. After pre-cold rolling to 3% reduction, the sample rolled along the TD and the sample rolled along the ND have similar tensile yield strength (~270 MPa). However, the former has a higher compressive yield strength, lower yield asymmetry and larger toughness than the latter. Moreover, pre-cold rolling can also enhance precipitation hardening effect. However, aging treatment cannot further improve the yield strength of pre-cold rolled samples. Finally, the related mechanism is discussed.

Key words: ZK60 alloy; pre-cold rolling; dislocation; twin; aging; mechanical properties

1 Introduction

It has been proven that plastic deformation is an effective method to enhance the mechanical properties of Mg alloys [1]. Traditional plastic processing techniques (e.g. rolling, extrusion and forging) have been used to develop wrought Mg alloys. To obtain better mechanical properties, further optimization of microstructure (e.g. ultrafine grains and weak texture) is required by developing new plastic deformation processes (e.g. severe plastic deformation and asymmetric plastic processing techniques) [1−3]. These new methods are effective to develop high-property Mg alloys, but require special equipment.

Recently, pre-deformation with low strain (e.g. pre-tension [4,5], pre-compression [6,7], pre-torsion [8,9], pre-shearing [10], pre-bending [11,12], pre-rolling [13,14], and pre-forging [15,16]) has been a popular method to tailor the mechanical properties of Mg alloys. These simple plastic deformations have some features, i.e., no special equipment required, and low plastic strain, thus receiving widespread attention. GONG et al [17] used pre-compression to improve the micro-hardness and wear resistance of a rolled ZK60 plate. KIM et al [6] and PARK et al [18] reported that pre-compression can regulate fatigue property and stretch formability of rolled AZ31 plates by inducing $\{10\bar{1}2\}$ twins. SONG et al [8] applied pre-torsion to reduce the yield asymmetry of an extruded AZ31 rod. CHEN et al [11] used pre-twinning to reduce the tension–compression yield asymmetry of a rolled ZK60 plate.

In addition, pre-cold deformation can also be

Corresponding author: Bo SONG, Tel: +86-23-68253204, E-mail: bosong@swu.edu.cn; Ren-long XIN, E-mail: rlxin@cqu.edu.cn
DOI: 10.1016/S1003-6326(21)65580-2

used to harden Mg alloys [19]. Cold deformation can introduce high density of crystal defects (e.g. dislocations, twin boundaries, and stacking faults) to generate defect hardening effect [20−22]. Moreover, it is also demonstrated that such defects might enhance the precipitation hardening effect of age-hardenable Mg alloys [5,7]. It is considered that the type of crystal defects may affect the hardening effect [19]. For wrought Mg alloys, the competition between slipping and twinning is largely dependent on strain path. In fact, previous researches have confirmed that strain path could determine the type of crystal defects. For rolled Mg alloy plates, pre-cold rolling along the normal direction (ND) can generate dislocations and contraction twins. However, pre-cold rolling along the transverse direction (TD) can introduce profuse extension twins [19]. Therefore, it is necessary to reveal the effects of strain path on defect hardening and aging hardening of Mg alloys. In this study, the material studied is a commercial ZK60 alloy, which has received widespread attention owing to its excellent plasticity and precipitation hardening effect [23,24]. Various pre-cold rolling paths were used to reveal different effects between dislocations and $\{10\bar{1}2\}$ twins on strength, toughness and yield asymmetry of a rolled ZK60 plate. Moreover, the necessity of aging is also discussed for pre-rolled ZK60 plates.

2 Experimental

The starting material for this study was an as-cast ZK60 (Mg−5.2wt.%Zn−0.5wt.%Zr) alloy. After homogenization at 400 °C for 24 h, the as-cast ZK60 alloy was hot-rolled to ~64% reduction of thickness at 300 °C. Then, the rolled sheet was subjected to solution treatments at 400 °C for 3 h. The rolled plate was cut into plates with dimensions of 40 mm (RD) × 10 mm (TD) × 8 mm (ND). Here, RD, ND and TD are the rolling direction, normal direction and transverse direction of the rolled plate, respectively. Subsequently, the ZK60 samples were subjected to pre-rolling at room temperature along various paths. To maintain a considerable plasticity, the low rolling reductions (<3%) were used to prepare the pre-rolled ZK60 plates. Figure 1 shows the paths of pre-cold rolling. Some samples were subjected to aging treatments at 175 °C for 10 h. In this study, six types of ZK60 sheets were prepared. The processing histories of six types of sheets are listed in Table 1. The samples were pre-rolled to thickness reductions of 1.5% and 3% (named as PRT 1.5% and PRT 3%, respectively, for the samples pre-rolled along the TD). Such abbreviations were also used in other samples.

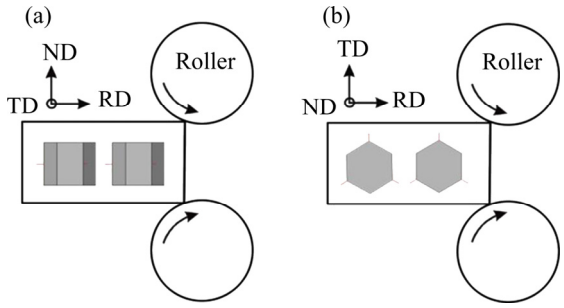

Fig. 1 Sketch map of pre-rolling: (a) Pre-rolling along ND; (b) Pre-rolling along TD

Table 1 Rolled ZK60 sheets subjected to various processing histories

Sample	Processing history
SS	As-solution rolled sheet (Original material)
SA	Direct aging
PRT	Pre-rolling along TD
PRTA	Pre-rolling along TD and then aging
PRN	Pre-rolling along ND
PRNA	Pre-rolling along ND and then aging

These samples were subjected to tension and compression tests along the RD. Dog-bone-shaped tension specimens with nominal gage dimensions of 8 mm × 3 mm × 1.5 mm and rectangular prism specimens with nominal dimensions of 4 mm × 4 mm × 8 mm were prepared. Mechanical tests were then carried out on an LD26.105 material test machine at a constant strain rate of 1×10^{-3} s^{-1}. The yield strength was measured as 0.2% proof stress. The extent of yield asymmetry was evaluated by calculating the ratio of compression yield stress (CYS) to tension yield stress (TYS). Each mechanical test was repeated at least three times to get representative results. The microstructure of the alloys was examined by electron backscatter diffraction (EBSD, Oxford AZtech Max2) analysis using an HKL Channel 5 System (Oxford system equipped in a JSM−6610). Transmission electron microscopy (TEM) observations were performed using a ZEISS Libra200FE microscope with accelerating voltage of 200 kV. The specimens for

TEM observations were ground with SiC paper and final thinning of the specimens was executed by a precision ion polishing system (GATAN691).

3 Results and discussion

3.1 Stress−strain curves of various samples

Figure 2 shows the true stress−strain curves of various samples. All tensile curves have a parabolic shape. In comparison, compressive curves present a concave shape which is a typical deformation feature dominated by $\{10\bar{1}2\}$ twinning [25]. To clearly illustrate the effect of pre-rolling, detailed mechanical properties and the variations of mechanical properties with pre-rolling strain are shown in Fig. 3. The plasticity (U_p) was evaluated by calculating the plastic strain corresponding to the peak strength. Figure 3(a) shows that tensile yield strength is higher than compressive yield strength for all samples. For SS sample, the yield strength is 209 and 113 MPa for tension and compression, respectively. Pre-rolling can enhance the yield strength of ZK60 plate, and pre-rolling path has a large influence on the hardening effect.

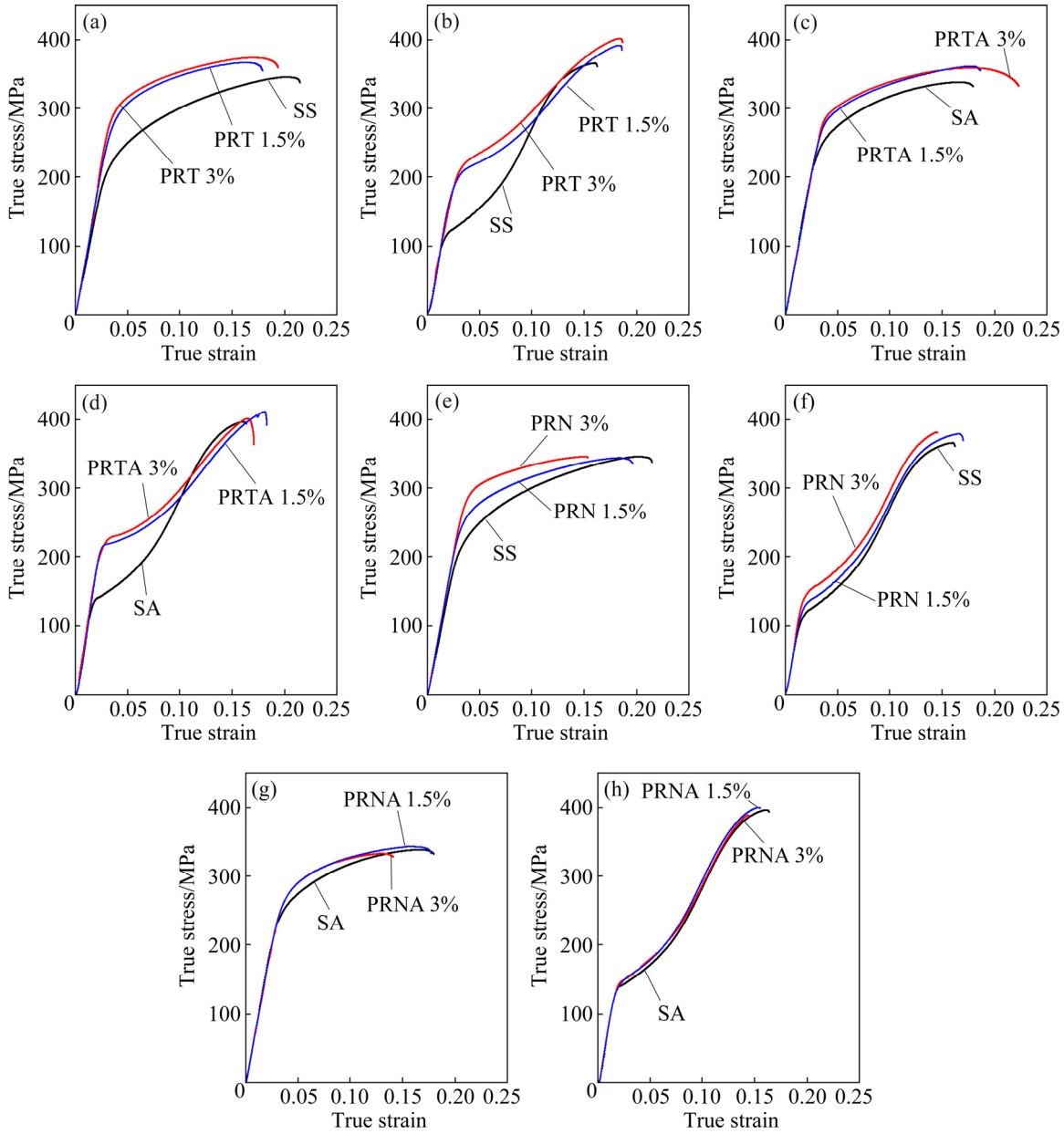

Fig. 2 Typical true stress−true strain curves of various samples deformed along RD: (a) Tensile curves of PRT samples; (b) Compressive curves of PRT samples; (c) Tensile curves of PRTA samples; (d) Compressive curves of PRTA samples; (e) Tensile curves of PRN samples; (f) Compressive curves of PRN samples; (g) Tensile curves of PRNA samples; (h) Compressive curves of PRNA samples

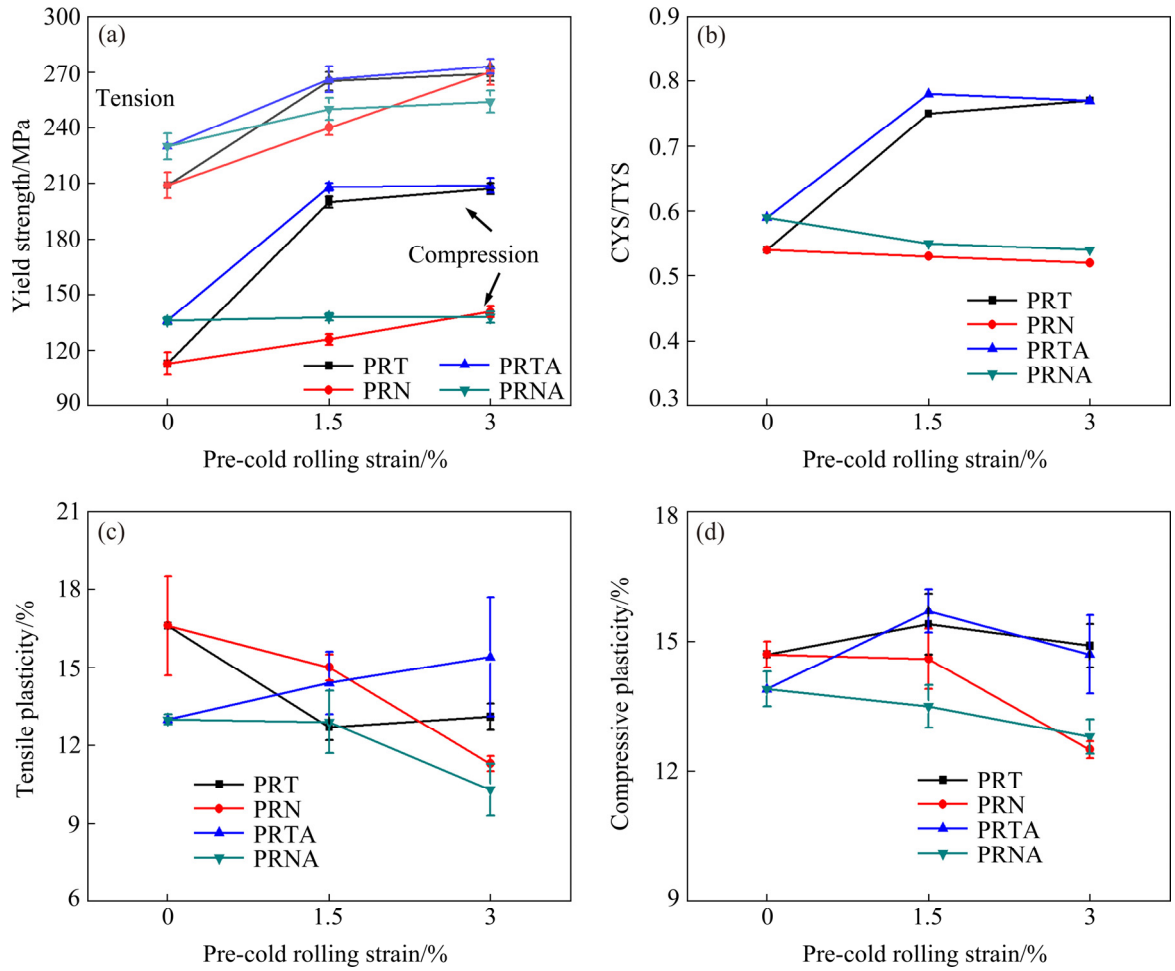

Fig. 3 Variations of mechanical properties along RD with pre-cold rolling strain: (a) Yield strength; (b) CYS/TYS; (c) Tensile plasticity; (d) Compressive plasticity

For pre-rolling along the ND, with increasing rolling strain from 1.5% to 3%, the tensile yield strength is increased by 31 and 61 MPa, and the compressive yield strength is increased by 13 and 28 MPa, respectively. Clearly, both tensile and compressive yield strengths exhibit a gradual increase with increasing pre-rolling strain. Moreover, PRN processing reduces plasticity (especially for tensile ductility). In contrast, it has little influence on CYS/TYS value and peak strength.

For pre-rolling along the TD, a pre-rolling strain of 1.5% can remarkably increase the yield strength along the RD (by 56 MPa for tension and by 87 MPa for compression). However, further increase in rolling strain to 3% exhibits insignificant effect on the yield strength. It is also found that PRT processing generates a higher hardening effect on compression than on tension, resulting in the improvement of yield asymmetry (see Fig. 3(b)). Moreover, PRT processing can also simultaneously enhance the peak strengths of tension and compression, as shown in Figs. 2(a) and 2(b), respectively. And PRT processing generates a smaller loss in tensile ductility compared with PRN processing.

Aging treatment can harden the yield strength of SS sample to 230 and 136 MPa for tension and compression, respectively. However, aging treatment does not necessarily further increase the yield strength of the pre-rolled ZK60 alloys, as shown in Fig. 3(a). For the PRT sample, aging treatment only slightly increases the tensile and compressive yield strengths. The increment is lower than 8 MPa. For the PRN sample, aging treatment makes the yield strength of the sample tend to a close value, i.e. ~250 MPa for tension and ~138 MPa for compression. In other words, aging treatment can increase the yield strength of PRN 1.5% sample, but it will reduce the yield strength of PRN 3% sample.

3.2 Influence of pre-rolling path on microstructure and yield strength

Figure 4 shows the EBSD maps and XRD pole figures of SS sample and the pre-rolled samples with a thickness reduction of 3%. Hot-rolling and following solution treatment lead to the formation of fine microstructure with an average grain size of about 10 μm and a strong basal texture, as shown in Fig. 4(a). After pre-rolling along the ND, only a small amount of twins can be formed and the basal texture is retained, as shown in Fig. 4(b). It is indicated that when rolling along the ND, dislocation slip is the dominant deformation mechanism instead of $\{10\bar{1}2\}$ twinning. Pre-rolling along the TD introduces a lot of twin lamellae, as shown in Fig. 4(c). EBSD data indicate that these twins are almost all $\{10\bar{1}2\}$ twins. The occurrence of $\{10\bar{1}2\}$ twinning causes grains to rotate by ~86°, resulting in a *c*-axis//TD texture in PRT sample [13].

In this study, Kernel average misorientation (KAM) was calculated to evaluate the dislocation accumulation [26]. KAM maps and average KAM values of various samples are also shown in Fig. 4. It is found that SS sample has a very low average KAM value (~0.63°). Pre-rolling increases the average KAM value to ~1.19° and ~0.87°, for PRN 3% sample and PRT 3% sample, respectively. It is indicated that PRN processing can generate higher dislocation accumulation than PRT processing. Based on EBSD data, the area fraction of $\{10\bar{1}2\}$ twins is ~28% and ~1.1% for PRT 3% sample and PRN 3% sample, respectively. Thus, the low dislocation accumulation in PRT sample can be attributed to the fact that $\{10\bar{1}2\}$ twinning has a large contribution to plastic strain of pre-rolling along the TD.

Clearly, the microstructure evolution during pre-rolling greatly depends on rolling path. As shown in Fig. 4(b), PRN 3% processing slightly increases basal texture intensity. Table 2 lists the mean Schmid factor (SF) for various deformation modes in different samples when loading along the RD. It is indicated that textural change via PRN 3% processing hardly affects yield strength. Thus, the increase in yield strength of PRN samples can be mainly attributed to the generation of dislocations during PRN processing. Initial dislocations can generate dislocation hardening effect. The relationship between yield increment via dislocation

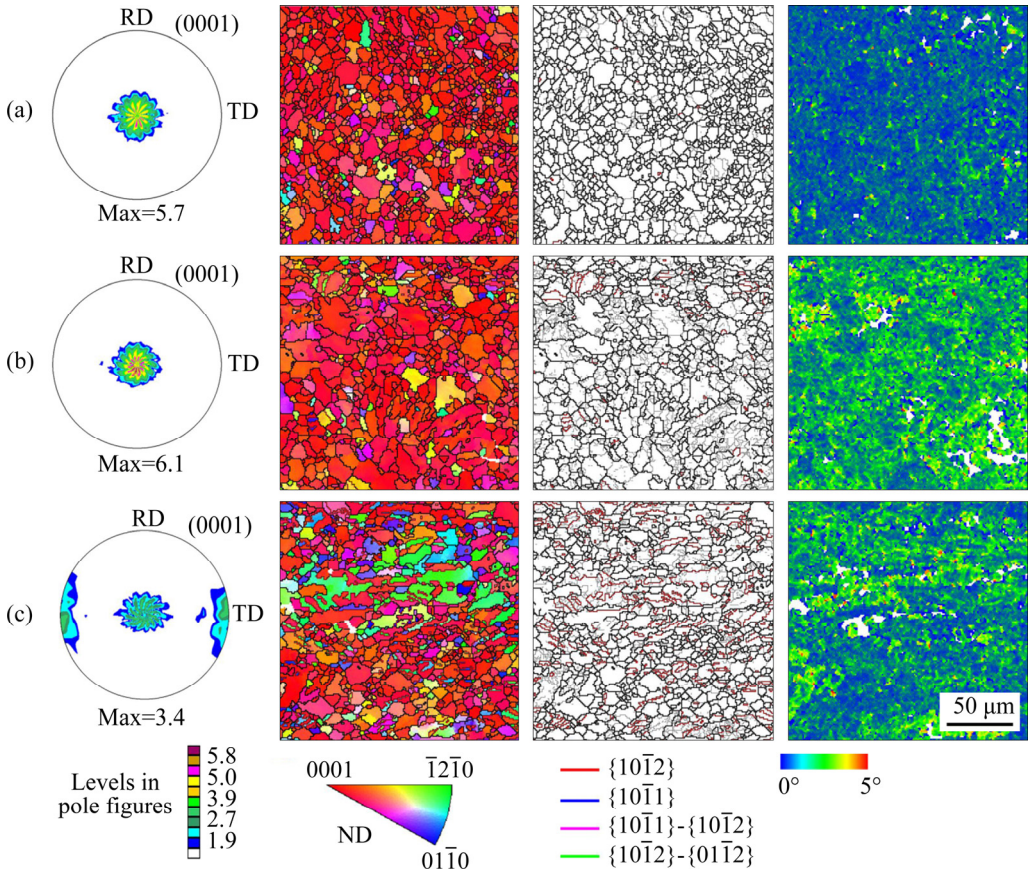

Fig. 4 XRD pole figure and EBSD maps of various samples: (a) SS sample; (b) PRN 3% sample; (c) PRT 3% sample

Table 2 Mean Schmid factor (SF) values for various deformation modes in different samples when loading along RD

Sample	Sate	Prismatic slip	$\{10\bar{1}2\}$ twinning	Basal slip
SS	Tension	0.435	0.027	0.195
	Compression		0.394	
PRN 3%	Tension	0.443	0.024	0.203
	Compression		0.397	
PRT 3%	Tension	0.424	0.043	0.243
	Compression		0.357	

hardening and dislocation density is usually represented as $\sigma_d=M\alpha Gb\rho^{1/2}$ (where ρ is total dislocation density, G is the shear modulus, b is the magnitude of Burgers vector, M is the Taylor factor and α constant) [27]. Clearly, σ_d is directly proportional to the dislocation density. Dislocation slip dominates the plastic strain for pre-rolling along the ND, as shown in Fig. 4(b). In this situation, the dislocation density will gradually increase with increasing rolling strain. It could be the reason why the yield strength of PRN sample gradually increases as the pre-rolling strain increases.

Compared with PRN sample, PRT sample contains profuse $\{10\bar{1}2\}$ twins, as shown in Fig. 4(c). The influence of initial twins on yield strength can be attributed to two aspects [28]. Firstly, $\{10\bar{1}2\}$ twinning can cause a lattice re-orientation of ~86.3° and generate a twin-texture. In the present work, a twin-texture with *c*-axis//TD is formed during PRT processing. Compared with initial *c*-axis//ND texture, the twin-texture has no influence on the orientation relationship between RD-loading and *c*-axis of texture. In fact, the *c*-axis of twin-texture has a slightly dispersion of ±30° from the TD towards the RD. The phenomenon was also observed by PARK et al [29]. Table 2 shows that the twin-texture can slightly increase the SF of basal slip for loading along the RD. It is indicated that the PRT processing can generate texture softening effect for loading along the RD. However, Fig. 3(a) indicates that the PRT processing generates a large hardening effect on yielding along the RD. It can be attributed to another effect of initial twins, i.e., twin-boundary hardening. It has been reported that $\{10\bar{1}2\}$ twins can subdivide grains, resulting in the refinement hardening effect [30]. It is considered that twin-boundary hardening has a main contribution to the increase of yield strength along the RD. As shown in Fig. 5(a), low rolling strain along the RD (1.5%) can generate profuse twin boundaries in matrix, thus remarkably increasing the yield strength (see Fig. 3). Figure 5(b) indicates that increasing rolling strain from 1.5% to 3% mainly causes twin-growth instead of nucleation of new twins. In fact, previous work [31,32] has revealed that $\{10\bar{1}2\}$ twins via rolling/compression along the TD nucleate at the beginning of plastic deformation (a strain of <2%). And twin-growth dominates subsequent plastic deformation [32,33]. Thus, with increasing rolling-strain from 1.5% to 3%, it is considered that the change in the number of twin boundaries may not be large, and thus yield strength exhibits little change (see Fig. 3(a)).

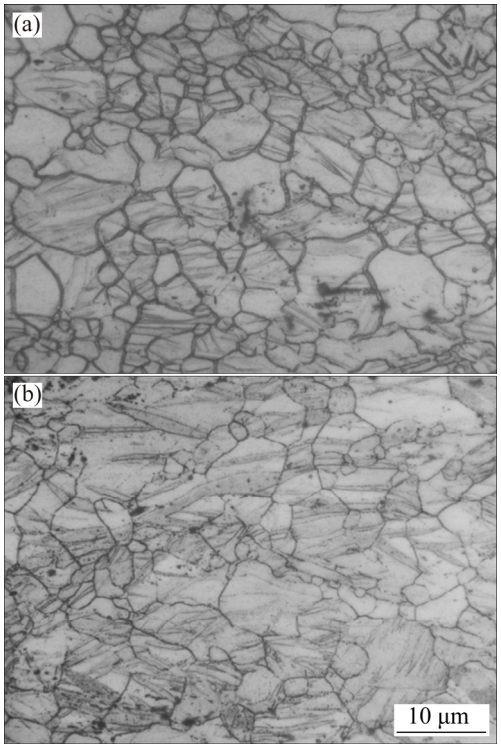

Fig. 5 Optical microstructure images of PRT samples: (a) PRT 1.5% sample; (b) PRT 3% sample

As shown in Fig. 4(c), KAM value can also be increased by PRT processing. Thus, dislocation hardening could also contribute to the increase of yield strength for PRT samples. The strain accommodated by twinning can be calculated as follows [34]:

$$\varepsilon_{twin}=f_{twin}\cdot SF_{twin}\cdot\gamma_{twin}$$

where ε_{twin}, f_{twin}, SF_{twin} and γ_{twin} represent the

twinning strain, the volume fraction of twins, the average SF of the twin variant, and the characteristic twinning shear, respectively. For $\{10\bar{1}2\}$ twinning in Mg alloys, γ_{twin} is known to be 0.13. When Schmid factor for $\{10\bar{1}2\}$ twinning chooses the maximum value (SF_{twin}=0.5), the maximum strain contributed by twinning can be calculated and is ~1.82% for PRT 3% sample. Thus, the strain of at least ~1.18% in PRT 3% sample is accommodated by dislocation slip. Thus, the effect of dislocation hardening on yielding of PRT sample cannot be ignored.

3.3 Influence of aging on microstructure and yield strength

Aging treatment was carried out to induce precipitation hardening effect. A common aging process (175 °C, 10 h) of ZK60 alloys is used in this work [23,24]. Figure 6 shows the EBSD maps of pre-rolled samples. Part of dislocations and all twin lamellae can be retained after aging. KAM maps show that aging treatment reduces the average KAM value to 0.77° and 0.92° for PRTA 3% sample and PRNA 3% sample, respectively. It is indicated that aging treatment generates a static recovery response.

In addition, aging treatment can also induce profuse precipitates in the matrix of ZK60 alloy. Figure 7 shows the TEM images with electron beam along the $[11\bar{2}0]$ direction. It is shown that disk-like β_2' precipitates are the major precipitates in the aged samples. The area fraction and number density (the number of precipitates per unit area) summarized by five TEM images with an area of 256036 nm^2 are shown in Table 3. After solution treatment, small amount of coarse precipitates retain in the matrix, as shown in Fig. 7(a). Aging treatment introduces a large number of fine precipitates, generating precipitation hardening effect to increase the yield strength of SS sample. It is also found that both PRN and PRT processing can increase the number density of β_2' phase during subsequent aging. According to previous reports [5,35], the dislocations via pre-cold rolling can provide heterogeneous nucleation sites for the precipitates. Thus, it is considered that

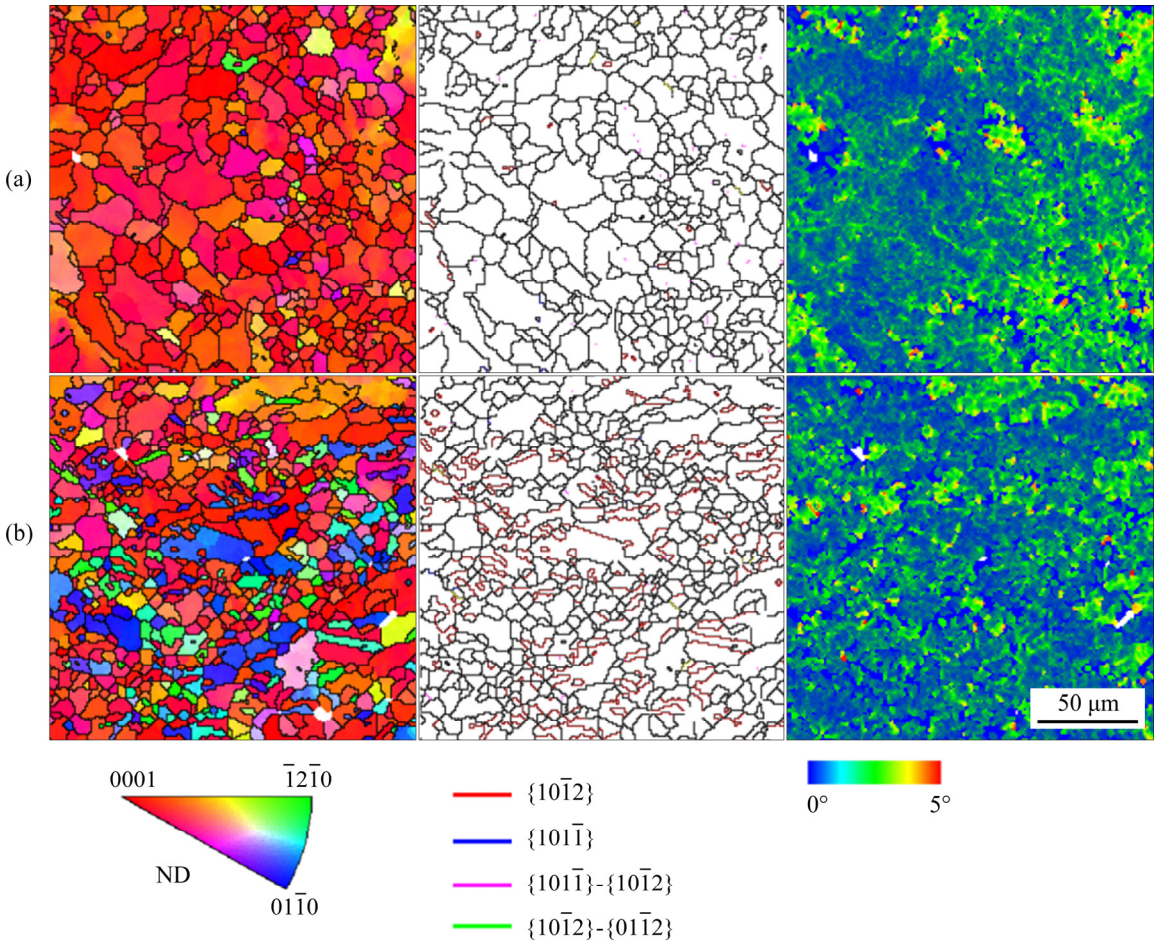

Fig. 6 EBSD maps of aged samples: (a) PRNA 3% sample; (b) PRTA 3% sample

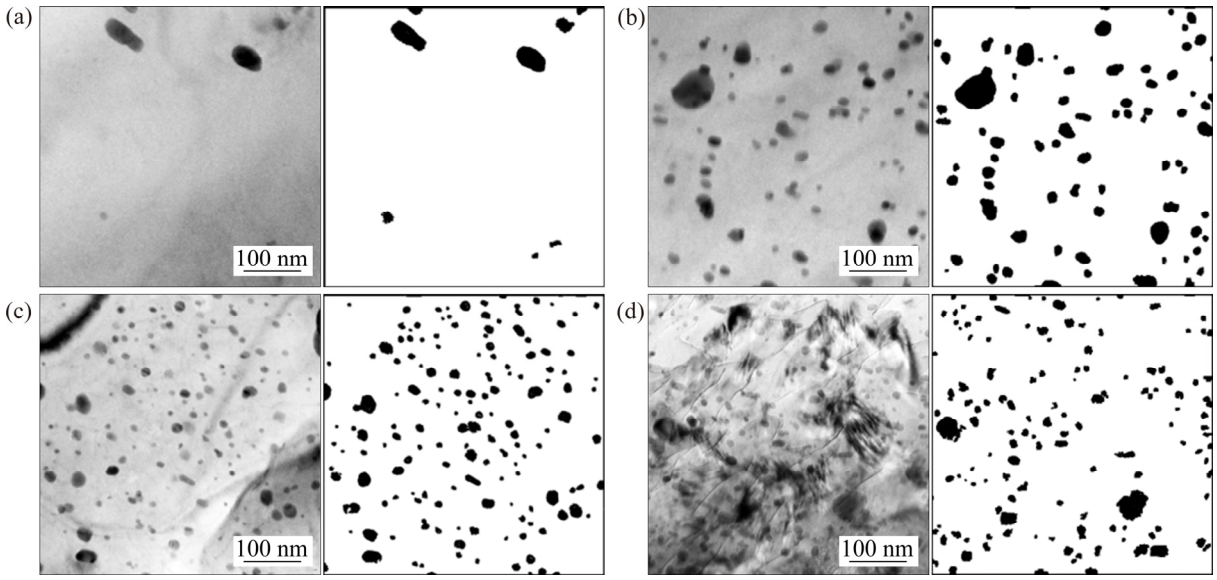

Fig. 7 TEM images with electron beam along $[11\bar{2}0]$ direction of Mg matrix (The right images are the corresponding sketches of the precipitates): (a) SS sample; (b) SA sample; (c) PRNA 3% sample; (d) PRTA 3% sample

Table 3 Area fraction and number density of precipitates in various aged samples

Sample	Area fraction/%	Number density/μm^{-2}
SS	1.9±0.5	31±11
SA	8.4±3.2	304±78
PRNA 3%	7.6±2.7	582±140
PRTA 3%	7.8±3.5	504±169

PRNA and PRTA samples have a higher precipitation hardening effect than SA sample. However, in fact, aging treatment only slightly increases the yield strength of PRT samples (<8 MPa), and even reduces the yield strength of PRN 3% sample. This is related to the softening effect via recovery of dislocations caused by aging. The reduction in dislocation density via aging can weaken dislocation hardening effect in pre-rolled samples. For PRT sample, the main hardening mechanism is refinement hardening via the subdivision of twin lamellae. Moreover, dislocations can also contribute to the increase of yield strength, as discussed above. Aging treatment only slightly increases the yield strength of PRT samples. It is indicated that the increment in yield strength via precipitation hardening is higher than that via dislocation hardening. In contrast, dislocation hardening is the main hardening mechanism in PRN sample. For PRN 1.5% sample, the initial dislocations can enhance the precipitation hardening effect. The increased precipitation hardening effect makes up the lack of dislocation hardening, resulting in higher yield strength than direct aging. However, with further increasing the pre-rolling strain, the contribution of dislocation hardening to yield strength increases. Thus, aging treatment can lead to a large loss of dislocation hardening. When precipitation hardening cannot compensate for the loss of dislocation hardening, aging will cause the decrease of yield strength. In fact, for the PRT sample with high pre-rolling strain, aging can also cause a reduction in yield strength, as reported by SONG et al [24].

3.4 Influence of pre-rolling path on yield asymmetry

Figure 3 shows that rolled ZK60 plate has a large tension−compression yield asymmetry. The CYS/TYS value is 0.54 for SS sample. It is well known that SF of specific slip system is equal for tension and compression with same loading axis. For all samples, prismatic slip has a very high SF value (>0.4), as shown in Table 2. In contrast, SF of basal slip is very low (~0.2). Unlike slip, due to the polar nature of twinning deformation, SF of $\{10\bar{1}2\}$ twinning under compression (>0.35) is far higher than that under tension (<0.03) (see Table 2). Previous work has revealed that the critical resolved shear stress (CRSS) of basal slip and $\{10\bar{1}2\}$ twinning is far lower than that of prismatic slip in ZK60 alloys [36]. However, basal slip cannot be the dominant deformation mechanism for

tension and compression due to its low SF. Moreover, the $\{10\bar{1}2\}$ twinning is strongly suppressed for tension along the RD. Thus, in this condition, the dominant deformation mechanism is prismatic slip and $\{10\bar{1}2\}$ twinning for tension and compression, respectively [37]. The large yield asymmetry can be attributed to the fact that the CRSS of prismatic slip is far larger than that of $\{10\bar{1}2\}$ twinning.

Table 4 lists the increment in yield strength and the change in CYS/TYS value caused by pre-rolling. It is found that pre-cold rolling can influence yield asymmetry. Table 2 indicates that pre-cold rolling does not change the dominant deformation mechanism for tension and compression. Thus, the change in yield asymmetry can be mainly attributed to the different hardening effects via pre-rolling on prismatic slip and $\{10\bar{1}2\}$ twinning. Table 4 also indicates that PRT and PRN samples exhibit different influence on yield asymmetry. PRT processing can remarkably reduce the yield asymmetry, but PRN processing slightly exacerbates yield asymmetry. As shown in Table 4, PRN 3% and PRT 3% processes generate a close increment in tensile yield strength (~61 MPa). However, they have a remarkably different hardening effect on the compressive yield strength, and the increment of compressive yield strength is 94 and 28 MPa for PRT 3% and PRN 3% processes, respectively.

Table 4 Increment of yield strength via different treatments

Sample	State	Increment of YS/MPa	CYS/TYS
SS	Tension	0	0.54
	Compression	0	
Aged	Tension	21	0.59
	Compression	23	
PRN 3%	Tension	61	0.52
	Compression	28	
PRNA 3%	Tension	45	0.54
	Compression	25	
PRT 3%	Tension	60	0.77
	Compression	94	
PRTA 3%	Tension	64	0.77
	Compression	96	

As discussed above, the main hardening mechanism is dislocation hardening and twin-boundary hardening for PRN and PRT samples, respectively. In fact, dislocation hardening can be evaluated by calculating the low-angle boundaries density with the misorientation angle ranging from 2° to 4° (LABs) [38]. Similarly, twin-boundaries (TBs) density is also calculated by EBSD data. The LABs density and TBs density are listed in Table 5. It is shown that LABs density in PRN 3% sample (0.133 μm^{-1}) is far higher than TBs density in PRT 3% sample (0.037 μm^{-1}). It is indicated that twin-boundary could generate a higher hardening effect on $\{10\bar{1}2\}$ twinning than low-angle boundary. Figure 8 shows the EBSD maps of the samples compressed to a strain of 3% along the RD. Extensive $\{10\bar{1}2\}$ twins are found in all compressed samples, which results in the formation of a twin-texture with *c*-axis//RD texture. Based on the orientation analysis, the area fraction of $\{10\bar{1}2\}$ twins via compression with a strain of 3% along the RD can be calculated. It is about 49%, 48% and 23% for the SS sample, PRN 3% sample and PRT 3% sample, respectively. Clearly, the effect of initial dislocations on twinning behavior is quite small in ZK60 alloys. In contrast, initial twins via pre-rolling along the TD can generate a strong inhibitory effect on the twin growth during compression along the RD. Two typical grains in PRN 3% and PRT 3% samples are shown in Fig. 9. In PRN 3% sample, profuse low-angle boundaries exist in matrix, as shown in Fig. 9(a). And a large orientation gradient can be found in the parent grain. It is shown that the low angle grain boundaries have little influence on twin growth. And the large orientation gradient can be evolved into the interior of the twins. For PRT 3% sample, both parent grains with *c*-axis//ND texture and the initial twins with *c*-axis//TD texture are favorable orientations

Table 5 LABs (2°−4°) density and TBs density in various samples

Sample	Density/μm^{-1}	
	LABs	TBs
SS	0.014	0.001
PRT 3%	0.072	0.037
PRTA 3%	0.055	0.039
PRN 3%	0.133	0.005
PRNA 3%	0.102	0.002

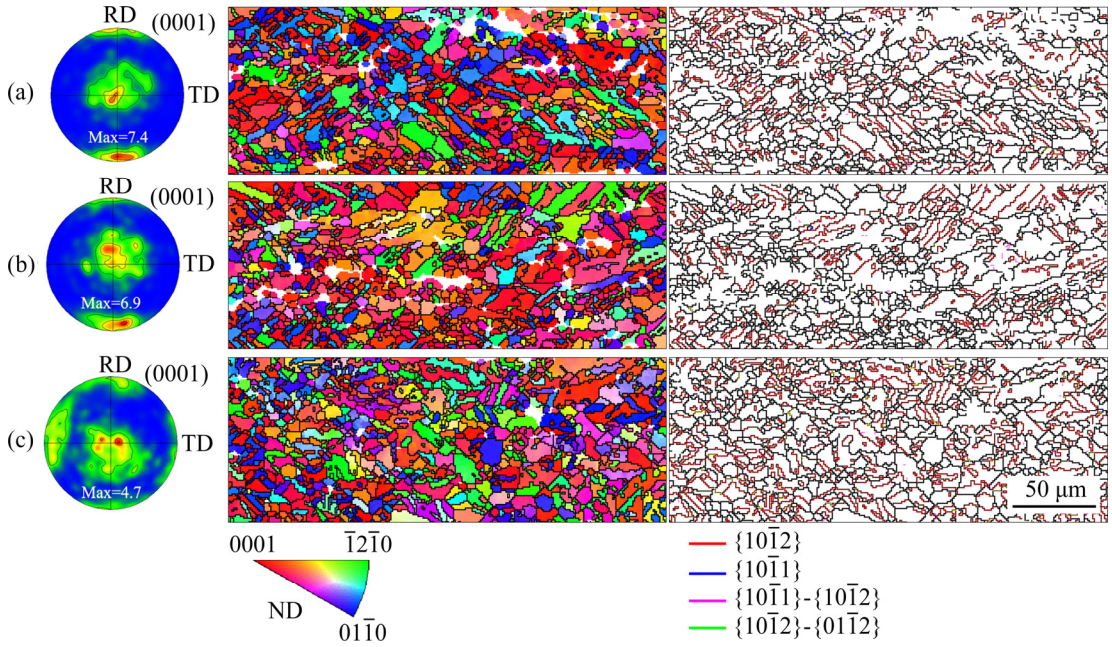

Fig. 8 EBSD maps of samples compressed to strain of 3%: (a) SS sample; (b) PRN 3% sample; (c) PRT 3% sample (Contour levels in pole figures are 2, 4, 6, ⋯)

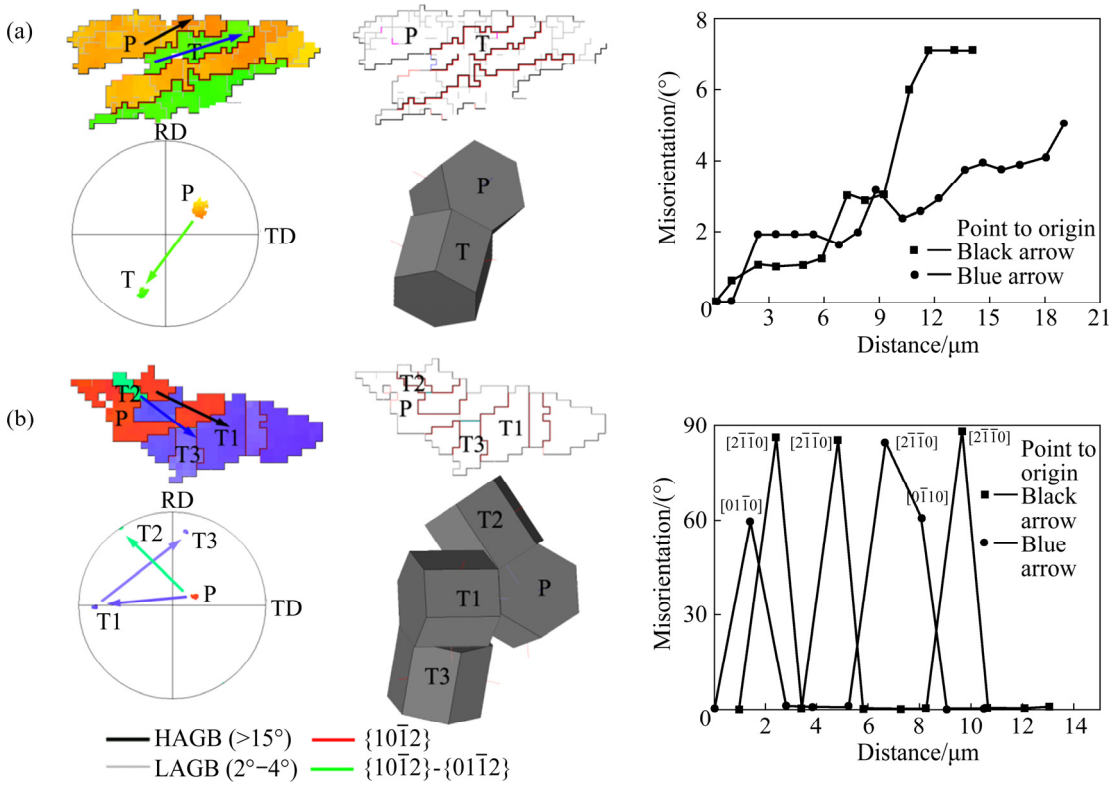

Fig. 9 Typical grains in samples compressed to strain of 3%: (a) PRN 3% sample; (b) PRT 3% sample (P and T represent parnent grain and twin, respectively)

for $\{10\bar{1}2\}$ twinning when the sample is compressed along the RD [13]. As shown in Fig. 9(b), the corresponding (0001) pole figure confirms that the T1 has an orientation close to the TD. It can be inferred that T1 is the initial twin produced during the pre-cold rolling along the TD. T2 and T3 are considered to be the $\{10\bar{1}2\}$ twins formed from parent grain and initial twin (T1),

respectively, during compression along the RD. It is noticeable that the growth of T2 and T3 is effectively limited by the twin boundaries of T1 generated by pre-rolling along the TD. The new 60°⟨10$\bar{1}$0⟩ boundaries can be formed (see blue arrow) and are not easy to migrate compared with 86.3°⟨11$\bar{2}$0⟩ twin boundaries [39]. In fact, YU et al [40] have found that the misorientation of grain boundary has a remarkable influence on hardening effect of {10$\bar{1}$2} twinning. With increasing misorientation between two neighbored grains, the hardening effect tends to increase. It is found that twin boundaries with a misorientation of 86.3° provide a higher hardening for {10$\bar{1}$2} twinning than that of GBs (0−50°) [40]. In the present work, it is also found the twin boundaries also generate a higher hardening effect on {10$\bar{1}$2} twinning than LABs. Thus, PRT 3% processing can significantly increase the compressive yield strength (by 94 MPa), while PRN processing only slightly increases it (by 28 MPa).

For refinement hardening via high-angle boundaries, BARNETT et al [41] has reported that the Hall−Petch slope (k value) for the twinning-dominated yield stress was higher than for slip-dominated yield stress. Thus, PRT processing can generate higher hardening effect on compression than on tension, resulting in the improvement of yield asymmetry. It is also found that dislocation hardening can largely make the dislocation movement hard, but it exhibits lower effect on twin-growth. The phenomenon is also observed in AZ31 alloy [13]. Its micro-mechanism is still unclear. In short, the high density of dislocations exacerbates yield asymmetry.

Aging treatment can also influence yield asymmetry. It is shown that direct aging slightly improves the yield asymmetry and increases the CYS/TYS value from 0.54 to 0.59. In fact, the influence of precipitates on yield asymmetry is dependent on the precipitate shape [37]. Previous work [23] has confirmed that disk-like β'_2 precipitates in ZK60 alloys can generate a slightly higher hardening effect on {10$\bar{1}$2} twinning than on prismatic slip. For PRT sample, not only does aging treatment generate a lot of disk-like β'_2 precipitates, but all twin boundaries can also be retained after aging. Thus, PRTA 3% sample maintains a low yield asymmetry (CYS/TYS=0.77). For PRN sample, both the formation of disk-like β'_2 precipitates and the loss of dislocations hardening are benefit for the improvement of yield asymmetry. However, the CYS/TYS value of PRNA 3% sample is only close to that of SS sample. In general, aging treatment exhibits little influence on yield asymmetry of PRT and PRN samples, and remarkably reduces the tensile yield strength of PRN 3% sample.

3.5 Influence of pre-rolling path on strain hardening and plasticity

To estimate the comprehensive mechanical properties, the static toughness (U_T) comprising both strength and ductility is summarized in Table 6. U_T is considered to be the total area under the true stress–strain curve, which is an indication of the amount of energy per unit volume that the material can absorb without rupturing [42]. For tension, both aging treatment and PRN processing can reduce the tensile ductility and static toughness. And combined use of PRN processing and aging can further reduce them. In contrast, PRT processing has little influence on static toughness. And subsequent aging can slightly increase the tensile ductility and static toughness of PRT 3% sample. It is well known that tensile ductility is related to strain hardening behavior [43]. Tensile strain hardening rate curves are shown in Figs. 10(a, b). To clearly evaluate the influence of pre-rolling on strain hardening

Table 6 Increment of various mechanical properties via different treatments

Sample	State	U_T/(MJ·m^{-3})	Increment of U_P/%
Solution-treated	Tension	61±6	0
	Compression	37±3	0
Aged	Tension	50±3	−3.6
	Compression	40±2	−0.8
PRN 3%	Tension	46±5	−5.3
	Compression	34±2	−2.2
PRNA 3%	Tension	39±6	−6.0
	Compression	33±2	−1.9
PRT 3%	Tension	61±5	−3.5
	Compression	53±2	0.2
PRTA 3%	Tension	63±7	−1.2
	Compression	47±3	−0.5

U_T−Static toughness

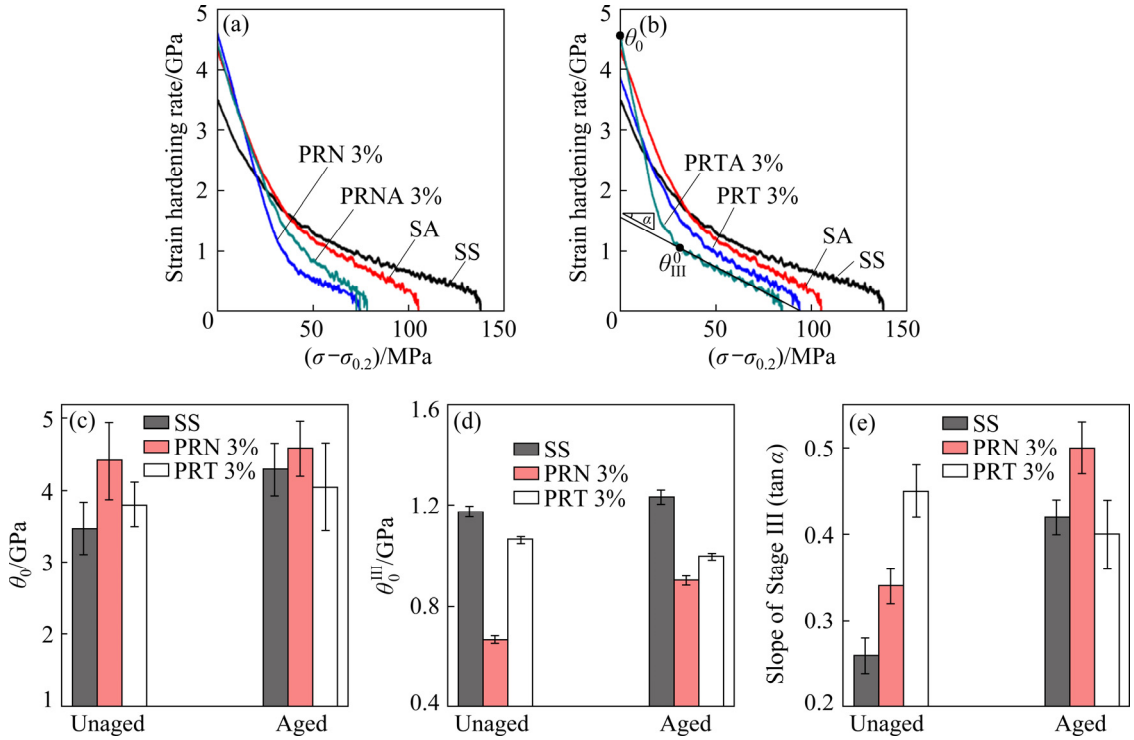

Fig. 10 Tensile strain hardening rate curves: (a, b) Strain hardening rate vs (σ−$\sigma_{0.2}$); (c) Initial hardening rate; (d) Initial hardening rate of Stage III; (e) Slope of Stage III hardening curves in tension

behavior, some important parameters (θ_0, θ_0^{III} and tan α) are shown in Figs.10(c−e). θ_0, θ_0^{III} and tan α represent the initial strain hardening rate, the initial strain hardening rate of Stage III and the slope of Stage III curve, respectively (taking the curve of PRTA 3% sample as an example in Fig. 10(b)). Initial hardening rate is related to the mobility of dislocations at yielding and the slope of strain hardening curve is associated with the dynamic recovery [43−46]. Figure 10 shows that after yielding, SS sample exhibits a slower transition from yielding to Stage III hardening, and also shows a higher θ_0^{III} (1174 MPa) and lower slope of Stage III (0.26) than other samples. Thus, SS sample remains high strain hardening rate within entire stress range during tension. It is reported that the maintenance of high strain hardening rate can retard tensile instability condition and contribute to high tensile ductility [43].

Both pre-rolling and aging can increase the initial hardening rate (θ_0). It is indicated that initial precipitates, dislocations and twin boundaries might be strong barriers to dislocation movement during yielding. Moreover, they may also promote the dislocation recovery to accelerate the reduction of strain hardening rate [43−46]. It is shown that direct aging has little influence on θ_0^{III}, but it enhances the slope of Stage III hardening curve (0.42). As reported by CHEN et al [44], numerous phase boundaries in ZK60 alloy can act as dislocation sinks, resulting in the increase of dynamic recovery during tension. In contrast, PRN processing largely accelerates the transition from yielding to Stage III hardening and largely reduces the θ_0^{III}. AFRIN et al [45] and SONG et al [13] found that initial dislocations may usually have taken part in the dislocation annihilation and enhanced dynamic recovery. It infers that the strong dislocation annihilation could result in a rapid decrease in hardening rate after yielding and a very low θ_0^{III} (667 MPa). PRN processing also slightly increases the slope of subsequent Stage III (0.34). Thus, PRN 3% sample exhibits very low level in strain hardening rate curve. For PRN 3% sample, aging treatment can remove part of dislocations (as shown in Fig. 6), thus resulting in the slight increase in θ_0^{III} (903 MPa). However, aging also generates numerous precipitates, which remarkably increases the slope of stage III hardening (0.5). Thus, aging and PRN processing reduce the tensile ductility. The decrease in ductility is also the main reason for the reduction of static toughness. The static

toughness is decreased from 61 to 50 and 46 MJ/m^3 for SA sample and PRN 3% sample, respectively. Aging treatment further reduces the yield strength and tensile ductility of PRN 3% sample, resulting in further reduction in the static toughness (to 39 MJ/m^3).

Unlike PRN 3% sample, PRT 3% sample contains abundant $\{10\bar{1}2\}$ twins and low density of dislocations, as shown in Fig. 4. It is reported that similar to grain boundaries, initial twin boundaries can reduce the θ_0^{III} [13]. However, the θ_0^{III} value in PRT 3% sample (1062 MPa) is far higher than that in PRN 3% sample. Although PRT processing increases the slope of Stage III hardening in PRT 3% sample (0.45), high θ_0^{III} value allows PRT 3% sample to maintain higher strain hardening rate and higher tensile ductility than PRN 3% sample. Previous report has found that the initial twin boundaries do not affect the slope of Stage III hardening [13]. The increase of slope of Stage III in PRT 3% sample can be attributed to the fact that initial dislocations via twinning deformation enhance the dynamic recovery during subsequent tension [13]. Moreover, it is also noted that the slope of Stage III hardening in PRT 3% sample with low density of dislocations is larger than that in PRN 3% sample with high density of dislocations. It is known that various rolling paths will generate different dislocation configurations, which might generate different effects on strain hardening behavior during tension. It is also found that subsequent aging slightly reduces the slope of Stage III (0.4). This could be the reason why PRTA sample remains high ductility. High ductility and high strength lead to a high static toughness in PRT 3% sample and PRTA 3% sample (61 and 63 MJ/m^3, respectively).

Compared with tension, aging and pre-rolling have a less influence on compressive plasticity, as shown in Table 6. For compression, $\{10\bar{1}2\}$ twinning dominates the plastic deformation at the early stage of plastic deformation [31]. Thus, strain hardening behavior of compression is closely related to the contribution of $\{10\bar{1}2\}$ twinning to plastic strain [46]. The strain hardening rate versus plastic strain curves are shown in Fig. 11. All curves exhibit a rapid elastic−plastic transition, and then enter a linearly increasing strain hardening behavior (Stage III). The increasing strain hardening rate in Stage III is mainly from texture hardening because twinning induces rotation of grains into hard orientations [25]. It is shown that both aging and PRN processing have little influence on strain hardening behavior. It is further proven that dislocations and precipitates have negligible influence on twin growth, as shown in Fig. 8. After the peak strain hardening rate is reached, slip will dominate subsequent deformation. Similar to tension, PRN processing results in a rapid drop in strain hardening rate in the late stage of deformation, which leads to a slight decrease in compressive plasticity.

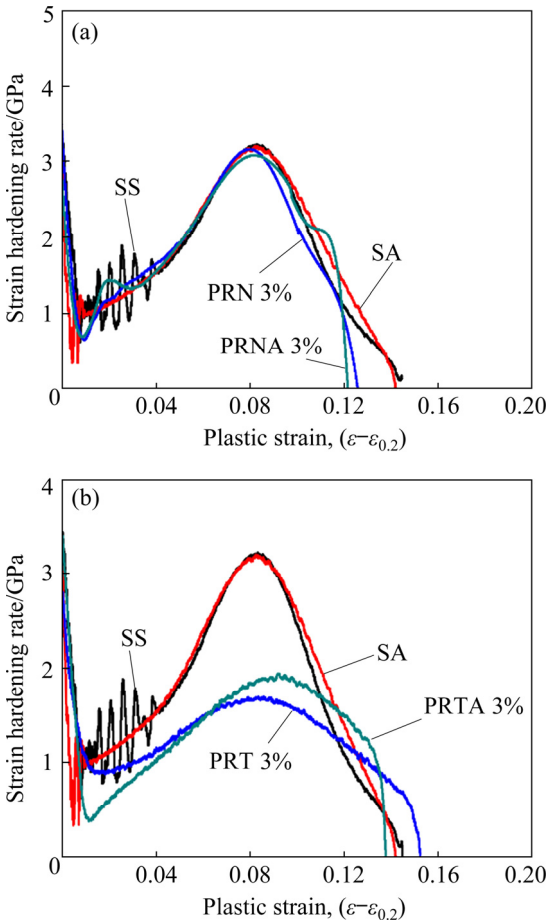

Fig. 11 Compressive strain hardening rate vs plastic strain curves: (a) PRN (PRNA) samples; (b) PRT (PRTA) samples

Figure 11(b) shows that PRT processing remarkably reduces the slope of Stage III and peak strain hardening rate. Table 2 and Fig. 8 indicate that PRT processing only delays twin-growth, and does not change the volume fraction of grains favorable for $\{10\bar{1}2\}$ twinning on compression along the RD. The low slope of Stage III in PRT sample could be attributed to the fact that initial twin boundaries decrease the contribution of

$\{10\bar{1}2\}$ twinning to unit strain at lower strain (<8%), as shown in Fig. 8. Moreover, the retardation of twinning activity also prolongs the Stage III curve [47]. Thus, in fact, the twinning deformation dominates a wider range of plastic strains in PRT 3% sample. Moreover, after the peak strain hardening rate, PRT (PRTA) sample exhibits a slower decrease in strain hardening rate than SS (SA) sample. Thus, initial twin boundaries have no obvious influence on the compressive plasticity.

Compared with tension, aging and pre-rolling have less influence on compressive plasticity. Thus, the static toughness of compression is more dependent on strength. Aging treatment can slightly increase the static toughness from 37 to 40 MJ/m^3. PRT processing can remarkably increase the stress−strain curves level, and thus the static toughness is increased to 53 and 47 MJ/m^3 for PRT 3% sample and PRTA 3% sample, respectively. In contract, PRN processing slightly decreases the static toughness to 34 MJ/m^3 owing to the loss of compressive plasticity, as shown in Table 6.

3.6 Necessity of aging for pre-rolled ZK60 plates

It is necessary to discuss the necessity of aging for pre-rolled ZK60 plates. As analyzed above, combined use of pre-cold rolling and aging can generate a larger hardening effect than direct aging. However, aging treatment does not necessarily play a positive role in the improvement of mechanical properties of pre-rolled ZK60 plate. For PRN processing, dislocation hardening is the main hardening mechanism. Aging treatment can remarkably weaken the dislocation hardening effect. It is also found that the PRN processing can enhance the precipitation hardening effect by promoting the nucleation of precipitates. Thus, the influence of aging treatment on yield strength is dependent on the competition between loss of dislocation hardening and increment in precipitation hardening. In the present work, it is also found aging treatment makes the yield strength of the PRN samples with various strains of pre-rolling tend to a close value. Thus, for little pre-rolling strains (e.g. 1.5%), aging can further enhance the yield strength. However, for high pre-rolling strain, aging can reduce the yield strength of PRN samples and is not beneficial to toughness (e.g. PRN 3% sample).

For PRT processing, twin-boundary hardening is main hardening mechanism. It is undeniable that dislocation strengthening has also a certain contribution to the increase in yield strength. Thus, aging treatment has a similar effect on PRN samples and PRT samples. In the present study, for a pre-rolling strain of less than 3%, subsequent aging can still slightly increase the yield strength. It has been reported that dislocation hardening has worse thermal stability than the aging hardening and twin boundary hardening [24]. Therefore, although the increment in yield strength via aging is very limited, it is considered that aging after PRT processing can enhance the thermal stability of PRT samples. Moreover, aging treatment exhibits little influence on yield asymmetry and plasticity of PRT samples. In this regard, aging is very necessary for PRT samples.

4 Conclusions

(1) Pre-cold rolling along the ND can generate a gradual increase in yield strength with increasing rolling strain from 1.5% to 3%. Compared with PRN 3% sample, PRT 1.5% sample has similar tensile yield strength and higher compressive yield strength. A further increase in the rolling strain from 1.5% to 3% only shows a slight increase in yield strength for PRT sample.

(2) The effect of pre-rolling path on hardening effect can be mainly attributed to different micro-structure evolutions between two rolling paths. Pre-cold rolling along the ND introduces numerous dislocations to generate dislocation hardening effect. In contrast, twin boundary hardening is the main hardening mechanism for PRT samples.

(3) Pre-cold rolling can enhance the precipitation hardening effect by promoting the nucleation of precipitates. However, aging treatment cannot further increase the yield strength of the pre-rolled ZK60 alloys. Aging treatment only slightly increases the yield strength of PRT 3% sample (by <4 MPa), and largely reduces the yield strength of PRN 3% sample (by 16 and 3 MPa for tension and compression, respectively).

(4) Pre-cold rolling along the ND slightly exacerbates yield asymmetry, and reduces static toughness (especially for tension). In contrast, pre-cold rolling along the TD remarkably increases the CYS/TYS value from 0.54 to 0.77, and increases the static toughness. Thus, pre-cold

rolling along the TD is more effective than pre-cold rolling along the ND in improving the comprehensive mechanical properties.

Acknowledgments

This work was financially supported by the National Natural Science Foundation of China (No. 51601154), the Fundamental Research Funds for the Central Universities, China (No. XDJK2019-B003), the Natural Science Foundation of Jiangsu Higher Education Institutions of China (No. 17KJD430006), and Chongqing Municipal Education Commission, China (No. KJZD-K202001502).

References

[1] CHEN Xiang, HUANG Guang-sheng, LIU Shuai-shuai, HAN Ting-zhuang, JIANG Bin, TANG Ai-tao, ZHU Yun-tian, PAN Fu-sheng. Grain refinement and mechanical properties of pure aluminum processed by accumulative extrusion bonding [J]. Transactions of Nonferrous Metals Society of China, 2019, 29(3): 437−447.

[2] LUO Xian, TAN Qi-yang, MO Ning, YIN Yu, YANG Yan-qing, ZHUANG Wyman, ZHANG Ming-xing. Effect of deep surface rolling on microstructure and properties of AZ91 magnesium alloy [J]. Transactions of Nonferrous Metals Society of China, 2019, 29(7): 1424−1429.

[3] WANG Qing-hang, SONG Jiang-feng, JIANG Bin, TANG Ai-tao, CHAI Yan-fu, YANG Tian-hao, HUANG Guang-sheng, PAN Fu-sheng. An investigation on microstructure, texture and formability of AZ31 sheet processed by asymmetric porthole die extrusion [J]. Materials Science and Engineering A, 2018, 720: 85−97.

[4] ZHANG Hua, HUANG Guang-sheng, WANG Li-fei, LI Jin-han. Improved formability of Mg–3Al–1Zn alloy by pre-stretching and annealing [J]. Scripta Materialia, 2012, 67(5): 495−498.

[5] HU Tong, XIAO Weng-long, WANG Fang, LI Yun, LYU Shao-yuan, ZHENG Rui-xiao, MA Chao-li. Improving tensile properties of Mg−Sn−Zn magnesium alloy sheets using pre-tension and ageing treatment [J]. Journal of Alloys and Compounds, 2018, 735: 1494−1504.

[6] KIM S H, HONG S G, LEE J H, LEE C S, YOON J, YU H, PARK S H. Anisotropic in-plane fatigue behavior of rolled magnesium alloy with $\{10\bar{1}2\}$ twins [J]. Materials Science and Engineering A, 2017, 700: 191−197.

[7] WANG Chun-peng, XIN Ren-long, LI Dong-rong, SONG Bo, WU Ming-yu, LIU Qing. Enhancing the age-hardening response of rolled AZ80 alloy by pre-twinning deformation [J]. Materials Science and Engineering A, 2017, 680: 152−156.

[8] SONG Bo, PAN Hu-cheng, CHAI Lin-jiang, GUO Ning, ZHAO Huai-zhi, XIN Ren-long. Evolution of gradient microstructure in an extruded AZ31 rod during torsion and annealing and its effects on mechanical properties [J]. Materials Science and Engineering A, 2017, 689: 78−88.

[9] WANG Jun, YANG Xu-yue, LI Yi, XIAO Zhen-yu, ZHANG Du-xiu, SAKAI T. Enhanced ductility and reduced asymmetry of Mg−2Al−1Zn alloy plate processed by torsion and annealing [J]. Transactions of Nonferrous Metals Society of China, 2015, 25(12): 3928−3935.

[10] PAN Hong-chen, WANG Feng-hua, FENG Miao-lin, JIN L, DONG J, WU P. Mechanical behavior and microstructural evolution in rolled Mg−3Al−1Zn−0.5Mn alloy under large strain simple shear[J]. Materials Science and Engineering A, 2018, 712: 585−591.

[11] CHEN Hong-bing, LIU Tian-mo, ZHANG Yin, SONG Bo, HOU De-wen, PAN Fu-sheng. The yield asymmetry and precipitation behavior of pre-twinned ZK60 alloy [J]. Materials Science and Engineering A, 2016, 652: 167−174.

[12] HABIBNEJAD-KORAYEM M, JAIN M K, MISHRA R K. Large deformation of magnesium sheet at room temperature by preform annealing. Part II: “Bending” [J]. Materials Science and Engineering A, 2014, 619: 378−383.

[13] SONG Bo, XIN Ren-long, CHEN Gang, ZHANG Xi-yan, LIU Q. Improving tensile and compressive properties of magnesium alloy plates by pre-cold rolling [J]. Scripta Materialia, 2012, 66(12): 1061−1064.

[14] JIANG Ji-miao, WU Jiang, NI Song, YAN Hong-ge, SONG Min. Improving the mechanical properties of a ZM61 magnesium alloy by pre-rolling and high strain rate rolling [J]. Materials Science and Engineering A, 2018, 712: 478−484.

[15] KIM Y J , KIM S H, LEE J U, CHOI J O, KIM H S, KIM Y, KIM Y, PARK S H. Effects of cold pre-forging on microstructure and tensile properties of extruded AZ80 alloy[J]. Materials Science and Engineering A, 2017, 708: 405−410.

[16] PARK S H, KIM H S, BAE J H, YIM C D, YOU B S. Improving the mechanical properties of extruded Mg–3Al–1Zn alloy by cold pre-forging [J]. Scripta Materialia, 2013, 69(3): 250−253.

[17] GONG Gui-lin, HUANG Guang-sheng, HUANG Lun, PAN Fu-sheng, JIANG Bin. Effect of compressive deformation on wear property of extruded ZK60 magnesium alloy [J]. Tribology Transactions, 2019, 62: 1−7.

[18] PARK S H, HONG S G, LEE C S. Enhanced stretch formability of rolled Mg–3Al–1Zn alloy at room temperature by initial $\{10\bar{1}2\}$ twins [J]. Materials Science and Engineering A, 2013, 578: 271−276.

[19] SONG Bo, SHE Jia, GUO Ning, QIU Ri-sheng, PAN Hu-cheng, CHAI Lin-jiang, YANG Chang-lin, GUO Sheng-feng, XIN Ren-long. Regulating precipitates by simple cold deformations to strengthen mg alloys: A review [J]. Materials, 2019, 12(16): 2507.

[20] IMANDOUST A, BARRETT C D, EL KADIRI H. Effect of rare earth addition on $\{10\bar{1}2\}$ twinning induced hardening in magnesium[J]. Materials Science and Engineering A, 2018, 720: 225−230.

[21] YU Hui-hui, XIN Yun-chang, CHENG Yao, GUAN Bo, WANG Mao-yin, LIU Qing. The different hardening effects of tension twins on basal slip and prismatic slip in Mg alloys [J]. Materials Science and Engineering A, 2017, 700: 695−700.

[22] LI Guo-qiang, ZHANG Jing-huai, WU Rui-zhi, LIU Shu-juan, SONG Bo, JIAO Yu-feng, YANG Qiang, HOU Le-gan. Improving age hardening response and mechanical properties of a new Mg−RE alloy via simple pre-cold rolling [J]. Journal of Alloys and Compounds, 2019, 777: 1375−1385.

[23] SONG Bo, XIN Ren-long, GUO Ning, XU Jian-bin, SUN Li-yun, LIU Qing. Dependence of tensile and compressive deformation behavior on aging precipitation in rolled ZK60 alloys [J]. Materials Science and Engineering A, 2015, 639: 724−731.

[24] SONG Bo, XIN Ren-long, SUN Li-yun, CHEN Gang, LIU Qing. Enhancing the strength of rolled ZK60 alloys via the combined use of twinning deformation and aging treatment [J]. Materials Science and Engineering A, 2013, 582: 68−75.

[25] KNEZEVIC M, LEVINSON A, HARRIS R, MISHRA R K, DOHERTY R D, KALIDINDI S R. Deformation twinning in AZ31 Influence on strain hardening and texture evolution [J]. Acta Materialia, 2010, 58: 6230−6242.

[26] BRITTON T B, BIROSCA S, PREUSS M, WILKINSON A J. Electron backscatter diffraction study of dislocation content of a macrozone in hot-rolled Ti–6Al–4V alloy [J]. Scripta Materialia, 2010, 62(9): 639−642.

[27] KOCKS U F, ARGON A S, ASHBY M F. Thermodynamics and kinetics of slip [J]. Progress in Materials Science, 1975, 19: 1−5.

[28] SONG Bo, GUO Ning, LIU Ting-ting, YANG Qing-shan. Improvement of formability and mechanical properties of magnesium alloys via pre-twinning: A review [J]. Materials & Design, 2014, 62: 352−360.

[29] PARK S H, HONG S G, LEE C S. In-plane anisotropic deformation behavior of rolled Mg–3Al–1Zn alloy by initial $\{10\bar{1}2\}$ twins [J]. Materials Science and Engineering A, 2013, 570: 149−163.

[30] TENG Jian-wei, GONG Xiao-juan, LI Yun-ping, NIE Yan. Influence of aging on twin boundary strengthening in magnesium alloys [J]. Materials Science and Engineering A, 2018, 715: 137−143.

[31] HONG S G, PARK S H, LEE C S. Role of $\{10\bar{1}2\}$ twinning characteristics in the deformation behavior of a polycrystalline magnesium alloy [J]. Acta Materialia, 2010, 58(18): 5873−5885.

[32] SONG Bo, XIN Ren-long, LIANG Yin-chun, CHEN Gang, LIU Qing. Twinning characteristic and variant selection in compression of a pre-side-rolled Mg alloy sheet [J]. Materials Science and Engineering A, 2014, 614: 106−115.

[33] LIU Ting-ting, YANG Qing-shan, GUO Ning, LU Yun, SONG Bo. Stability of twins in Mg alloys—A short review [J]. Journal of Magnesium and Alloys, 2020, 8(1): 66−77.

[34] ROBERTS C S. Magnesium and its alloys [M]. New York: John Wiley, 1960.

[35] LAI Y X, FAN W, YIN M J, WU C L, CHEN J H. Structures and formation mechanisms of dislocation-induced precipitates in relation to the age-hardening responses of Al−Mg−Si alloys [J]. Journal of Materials Science & Technology, 2020, 41: 127−138.

[36] REN Wei-jie, XIN Ren-long, XU Jian-bin, SONG Bo, ZHANG Ling, LIU Qing. Effects of precipitate type on twin/slip activity in ZK60 alloys and yield asymmetry [J]. Journal of Alloys and Compounds, 2019, 792: 610−616.

[37] ROBSON J D, STANFORD N, BARNETT M R. Effect of precipitate shape on slip and twinning in magnesium alloys [J]. Acta Materialia, 2011, 59(5): 1945−1956.

[38] WANG Mao-yin, XIN Ren-long, WANG Bing-shu, LIU Qing. Effect of initial texture on dynamic recrystallization of AZ31 Mg alloy during hot rolling [J]. Materials Science and Engineering A, 2011, 528: 2941−2951.

[39] CHEN Peng, WANG Fang-xi, OMBOGO J, LI Bin. Formation of 60° $\langle 0\bar{1}10\rangle$ boundaries between $\{10\bar{1}2\}$ twin variants in deformation of a magnesium alloy [J]. Materials Science and Engineering A, 2019, 739: 173−185.

[40] YU hui-hui, XIN Yun-chang, CHAPUIS A, HUANG Xiao-xu, XIN Ren-long, LIU Qing. The different effects of twin boundary and grain boundary on reducing tension-compression yield asymmetry of Mg alloys [J]. Scientific Reports, 2016, 6: 29283.

[41] BARNETT M R, KESHAVARZ Z, BEER A G, ATWELL D. Influence of grain size on the compressive deformation of wrought Mg–3Al–1Zn [J]. Acta Materialia, 2004, 52(17): 5093−5103.

[42] HOSFORD W F. Mechanical behavior of materials [M]. New York: Cambridge University Press, 2005.

[43] DEL VALLE J A, CARREÑO F, RUANO O A. Influence of texture and grain size on work hardening and ductility in magnesium-based alloys processed by ECAP and rolling [J]. Acta Materialia, 2006, 54: 4247−4259.

[44] CHEN Xian-hua, PAN Fu-sheng, MAO Jian-jun, WANG Jing-feng, ZHANG Ding-fei, TANG Ai-tao, PENG Jian. Effect of heat treatment on strain hardening of ZK60 Mg alloy [J]. Materials & Design, 2011, 32(3): 1526−1530.

[45] AFRIN N, CHEN D L, CAO X, JAHAZI M. Strain hardening behavior of a friction stir welded magnesium alloy [J]. Scripta Materialia, 2007, 57(11): 1004−1007.

[46] SONG Bo, XIN Ren-long, GUO Ning, LIU Ting-ting, YANG Qing-shan. Research progress of strain hardening behavior at room temperature in wrought magnesium alloys [J]. The Chinese Journal of Nonferrous Metals, 2014, 24: 2699−2710. (in Chinese)

[47] WANG Bing-shu, XIN Ren-long, HUANG Guang-jie, LIU Qing. Effect of crystal orientation on the mechanical properties and strain hardening behavior of magnesium alloy AZ31 during uniaxial compression [J]. Materials Science and Engineering A, 2012, 534: 588−593.

预轧制路径对 ZK60 镁合金力学性能的影响

宋 波[1]，杜治文[1]，杨青山[2]，郭 宁[1]，郭胜锋[1]，于金程[3]，辛仁龙[4]

1. 西南大学 材料与能源学院，重庆 400715；
2. 重庆科技学院 冶金与材料工程学院，重庆 401331；
3. 无锡职业技术学院 机械技术学院，无锡 214121；
4. 重庆大学 材料科学与工程学院，重庆 400044

摘 要：采用低轧制压下量的预冷轧(<3%)来改善轧制 ZK60 板的力学性能。详细研究轧制路径对力学性能的影响。沿横向的预冷轧和沿法向的预冷轧均可提高屈服强度。但是，在改善综合力学性能方面，沿横向预冷轧比沿法向预冷轧更为有效。预冷轧 3%的压下量后，沿横向轧制的样品和沿法向轧制的样品具有相近的拉伸屈服强度（～270 MPa）。但是，前者比后者具有更高的压缩屈服强度、更低的屈服不对称性和更好的韧性。此外，预冷轧还可以增强沉淀硬化效果。但是，时效处理不能进一步提高预冷轧样品的屈服强度。最后，讨论相关的机理。

关键词：ZK60 合金；预冷轧；错位；孪晶；时效；力学性能

(Edited by Bing YANG)